A flexible lid controls access to the active site in 1,3,8-trihydroxynaphthalene reductase

Arnold Andersson[a], Douglas Jordan[b], Gunter Schneider[c], Ylva Lindqvist[c,*]

[a]*Department of Molecular Biology, Swedish University of Agricultural Sciences, Uppsala Biomedical Center, PO Box 590, S-75124 Uppsala, Sweden*
[b]*Dupont Agricultural Products, Stine-Haskell Research Center, Box 30, Elkton Road, Newark, DE 19714, USA*
[c]*Department of Medical Biochemistry and Biophysics, Karolinska Institute, S-171 77 Stockholm, Sweden*

Received 28 October 1996

Abstract The crystal structures of apo-1,3,8-trihydroxynaphthalene reductase from *Magnaporthe grisea* and a binary complex of the enzyme with NADPH have been determined to 2.8 Å resolution. In both cases, the overall structure is preserved compared to the structure of the ternary complex of the enzyme with NADPH and an active site inhibitor. No electron density for the helix–loop–helix region comprising residues 214–244 is observed indicating structural disorder in this part of the apoenzyme and the binary complex. In the ternary complex, this region is in contact with NADPH and the inhibitor and closes off the active site. The observed increase in flexibility in the absence of the inhibitor indicates that this region acts as a lid which closes the active site upon binding of the inhibitor and, possibly the substrate, 1,3,8-trihydroxynaphthalene.

Key words: Rice blast; Naphtol reductase; Protein crystallography; Short-chain dehydrogenase

1. Introduction

Magnaporthe grisea, the determinant of rice blast disease, is a fungus that utilizes melanin-coated appressoria to directly penetrate rice leaf epidermal cells. The fungal melanin is essential for creating sufficiently high hydrostatic pressure in the appressoria to allow penetration of the leaf cells [1].

One of the enzymes in the biosynthesis of melanin in *M. grisea* is the homotetrameric enzyme 1,3,8-trihydroxynaphthalene reductase (THNR), which catalyses the conversion of 1,3,8-trihydroxynaphthalene to vermelone. Two other enzymes of the melanin pathway have been characterized: scytalone dehydratase [2] and 1,3,6,8-tetrahydroxynaphthalene reductase (Jordan, D., unpublished results).

The enzyme subunit of THNR from *M. grisea* consists of 283 residues with a molecular weight of 30 kDa [3]. The 3-dimensional structure of the enzyme in complex with NADPH and an active site inhibitor has recently been determined at 2.8 Å resolution [4] establishing that it is a member of the short-chain dehydrogenase family. The enzyme contains the sequence characteristics of this family; a GXXXGXG motif found close to the dinucleotide binding site, and a Ser–Lys–Tyr triad. Extensive contacts between the subunits of the tetramer are made at two different interfaces. At one of these interfaces, a four-helix bundle is formed. At the second interface, two parallel seven-stranded β-sheets are arranged antiparallel to each other forming a 14-stranded bowl-shaped β-sheet. A diagram of the tertiary structure of the *M. grisea* THNR is shown in Fig. 1 where the two regions contributing to these interfaces are indicated.

Each catalytic cycle involves the binding and release of substrates and products. For this to occur, one or more regions of the enzyme must move to allow access to the completely buried active site; the accessible surface area of the inhibitor in the ternary complex was calculated to be 0 Å^2 [4]. In this report we present the crystal structures of trihydroxynaphtalene reductase in its apo-form and in complex with NADPH and compare these structures to the structure of the ternary complex THNR–NADPH–inhibitor. This study identifies one protein region close to the active site as flexible and suggests that this helix–loop–helix motif might act as a lid which covers the active site upon binding of the substrate.

2. Materials and methods

2.1. Crystallization

Recombinant THNR was prepared as described previously [5]. Crystals of the apoenzyme were grown at 4°C by the hanging drop method using a well solution of 1.6 M $(NH_4)_2SO_4$ buffered to pH 6.0 with 0.1 M MES (2-[*N*-morpholino]ethanesulfonic acid). These crystals belong to the space group $P3_121$ with cell dimensions $a = b = 142.1$ Å and $c = 69.8$ Å. Crystals of the holoenzyme were grown at 4°C by the hanging drop method under similar conditions as the ternary complex [5] (but no inhibitor had been added) using a well solution of 19% polyethylene glycole 6000 buffered to pH 7.2 with 0.1 M HEPES (*N*-[2-hydroxyethyl]piperazine-*N*′-2-ethane sulfonic acid). The holoenzyme crystals belong to the space group $P3_121$ with cell dimensions $a = b = 143.3$ Å and $c = 71.2$ Å. All crystal forms contain two molecules in the asymmetric unit.

2.2. Data collection

Before data collection, a crystal of the apoenzyme was soaked 1 min in crystallization buffer containing 20% (v/v) ethylene glycole, and then flash-frozen under a nitrogen gas stream at 100 K. X-ray data for the binary complex were collected at 4°C. Data-sets for crystals of the apoenzyme and the binary complex were collected with an R-axis II image plate mounted on an Rigaku rotating anode. The data sets were processed using DENZO [6] and were scaled and merged using the CCP4 program package [7]. Statistics for these data sets are given in Table 1.

2.3. Structure determination

All crystallographic refinement was done with the program X-PLOR [8] using Engh and Huber parameters [9]. Due to the medium resolution of the X-ray data, the coordinates of the two subunits in the aymmetric unit were constrained by the non-crystallographic symmetry.

The model of the apoenzyme was refined using the structure of the ternary complex as starting model (NADPH and inhibitor were not included in the model). These coordinates were subjected to rigid-body refinement, energy minimization, simulated annealing and manual rebuilding using O [10] and a second round of energy minimization. This reduced the R-factor from the initial 44.9% to 33.2%. Due to an anisotropic diffraction pattern, an anisotropic correction was applied to the observed structure factors [11]. In the initial stages of

*Corresponding author. Fax: (46) 8-32-76-25.

Abbreviations: THNR, 1,3,8-trihydroxynaphthalene reductase

PII S0014-5793(96)01382-8

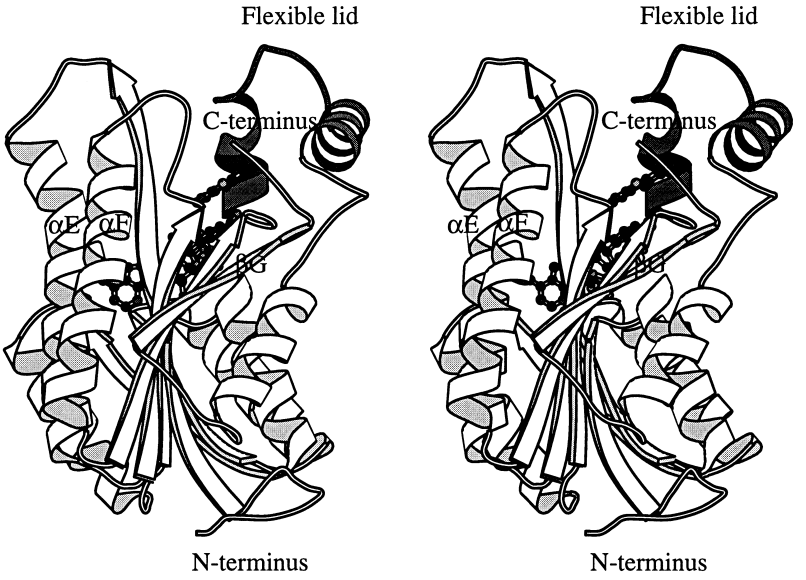

Fig. 1. Schematic view of THNR with bound NADPH and inhibitor shown as ball-and-stick models. The secondary structure elements αE, αF and βG involved in tetramer formation are labeled. The α1–loop–α2 region acting as a flexible lid is shaded dark. The figure was produced with the program MOLSCRIPT [15].

the refinement, an overall B-factor was used, but in the last cycles, a grouped B-factor refinement was included. The final model has an R-factor of 27.5% (R-free 31.1%) for 17318 unique reflections in the resolution range between 8.0 and 2.8 Å (Table 2). Due to the relatively high residual R-values of the model, molecular replacement using AMoRe [12] was applied to verify that the model was not stuck in a local energy minimum. The refined structure of the ternary complex (coenzyme and inhibitor were not included) was used as search model and the best solution gave the same orientation and position as the refined structure of the apoenzyme based on difference Fourier methods.

Refinement of the binary complex started from the coordinates for the model of the ternary complex, without the inhibitor. The protocol for the crystallographic refinement followed that outlined above for the apoenzyme and the final R-factor was 24.9% (R-free 28.5%) for 17172 unique reflections (Table 2).

The refined protein models were analyzed with PROCHECK [13]. Structural superpositions were carried out using the LSQ option in the program O [10].

3. Results and discussion

3.1. Electron density map and crystal packing

The electron density maps for apo-THNR and the binary complex are well defined except for three regions. No electron density can be observed for the first 15 residues at the N-terminus, and for residues 213–244. Only poor electron density is found for the region comprising residues 167–170.

The crystals of apo-THNR and the THNR–NADPH complex are not isomorphous to each other nor to the crystals of the ternary complex of THNR–NADPH–inhibitor. These crystal forms belong to the same space group, but they show differences in cell dimensions, in particular in the length of the c-axis. The differences might be caused by small changes in the packing interactions between the tetramers giving rise to an approximate 0.8 Å translation along the c-axis relating one subunit of the apo- and holoenzyme to the position of the subunit in the ternary complex. Packing of tetramers involves four surface areas, made up of loops between secondary structure elements αB–βB, αC–βC and αD–βD from one subunit and loops between secondary structure elements αD–βD, αE–βE and αF–βF from a subunit in the adjacent tetramer. The interactions consist of van der Waals contacts and two possible hydrogen bonds (Lys^{55}–Glu^{154} and Asp^{80}–Lys^{199}). Only 400 $Å^2$ of accessible surface area is buried at each tetramer interface which could be one explanation for the observed non-isomorphism among the three crystal forms.

3.2. Overall structures

The structures of apo- and holoenzyme are very similar to that of the ternary complex (THNR–NADPH–inhibitor). Least-squares superposition of the Cα coordinates for the subunit of the apoenzyme or the binary complex to the structure of the ternary complex resulted in an r.m.s. deviation of 0.57 Å in both cases (using Cα atoms 15–212 and 245–283). Superposition of the apo- and holoenzyme structures gave an r.m.s. deviation of 0.47 Å, using the same range of Cα atoms. These differences in structures are evenly distributed along the chain and are within the error of the model at this resolution. No significant differences in the packing of the subunits within the tetramer were found which indicates that binding of the inhibitor does not induce changes in the quaternary structure large enough to be detected at the present resolution.

3.3. Active site regions

Examination of the electron density maps of the aopenzyme

Table 1
Statistics of data collection

Data set	Apoenzyme	Holoenzyme
Resolution	2.8 Å	2.8 Å
No. of observed reflections	96605	71496
No. of unique reflections	18407	18202
Completeness (%)	90.9	87.8
Multiplicity	5.3	3.9
Rsym	0.082	0.097

Table 2
Model refinement parameters

	Apoenzyme	Holoenzyme
Resolution range	8–2.8 Å	8–2.8 Å
No. of non-hydrogen atoms	1745	1778
No. of reflections	17318	17172
R-factor	27.5%	24.9%
Free R-factor	31.1%	28.5%
Root mean square deviation in:		
Bond lengths (Å)	0.011	0.012
Bond angles (°)	1.9	2.2
Mean B-value (Å^2)	33.8	33.7
Ramachandran plot:		
% of non-glycine residues in the most favorable (disallowed) regions:	88.8 (0)	89.8 (0)

and the binary complex showed, with the exception of the flexible regions 167–170 and 213–244 (see below) no local changes in the protein structure in the active site region.

The Fo-Fc electron density map of apo-THNR revealed positive electron density at 8 times the standard deviation of the map close to the position of the adenosine ribose 2′ phosphate group of NADPH in the binary and ternary complexes. Since the crystallization buffer contained 1.6 M $(NH_4)_2SO_4$, this electron density was modeled by a sulphate-ion (Fig. 2).

In the electron density map calculated from data for the binary complex there is clear electron density for the adenine, the adenine ribose and the pyrophosphate group of the dinucleotide. However, there is no electron density corresponding to the nicotinamide ring and the nicotinamide ribose, indicating that this part of the molecule is disordered in the crystals. Similar observations have been made previously, for instance in the structure of the complex of dihydrofolate reductase with $NADP^+$ [14] where only the adenosine and ribose part of the dinucleotide was defined in its electron density. In the structure of the ternary complex of THNR, the nicotinamide ring forms hydrogen bonds with two residues of the disordered part, Ile^{211} and Thr^{213} and the absence of these interactions might in part be responsible for the local disorder of the nicotinamide ring of NADPH.

3.4. Flexible lid at the active site

The major differences between the structure of the THNR–NADPH–inhibitor complex to the structures of the apoenzyme and the THNR–NADPH complex reside in the region including residues 213–244 which is flexible in the apoenzyme and the binary complex. In the structure of the ternary complex, this region forms a helix–loop–helix motif which folds over the active site and interacts with the dinucleotide and the inhibitor (Fig. 1). Residues Met^{215}, Val^{219}, Cys^{220}, Tyr^{223}, and Trp^{243} form part of the substrate binding pocket and are close to atoms of the inhibitor. In particular the side chain of Tyr^{223} forms an important stacking interaction between the aromatic rings of the protein side chain and the inhibitor, and possibly the substrate in an analogous fashion. It seems that the numerous van der Waals and hydrophobic interactions between this region of the protein and the substrate are required to order the structure of this part of the active site. The α1–loop–α2 part of THNR therefore might act as a lid which closes over the active site upon binding of substrate.

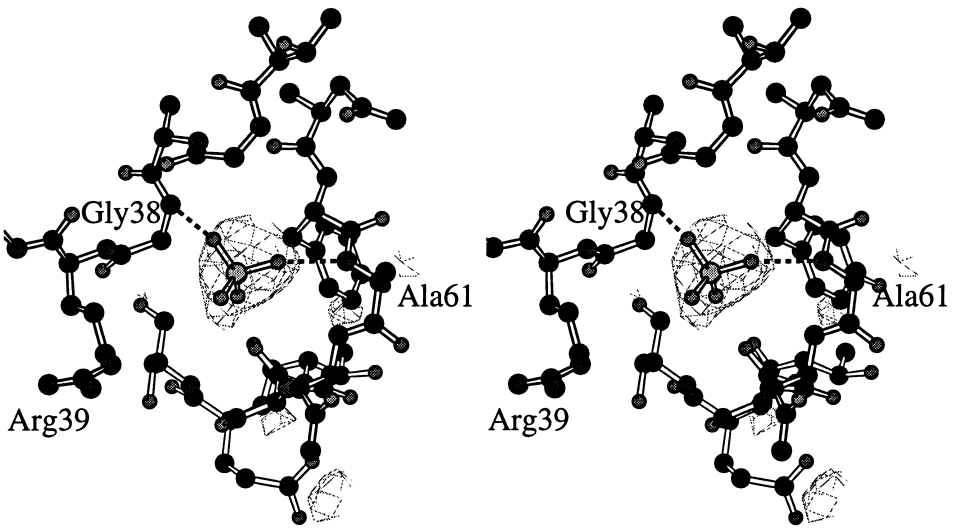

Fig. 2. Part of a Fo-Fc difference electron density map calculated with phases derived from the refined model of the apoenzyme and contoured at 3 σ, showing the region around the bound sulphate-ion. The sulphate ion had been omitted from the phase calculation. The two possible hydrogen bonds between two oxygen atoms of the sulphate ion and the peptide NH groups of Gly^{38} and Ala^{61} are shown as dashed lines. The figure was produced with the program MOLSCRIPT [15].

Part of the loop (residues 167–170) between βE and αF which is closing off parts of the active site in the ternary complex also shows poor electron density in both the apo- and holoenzyme structures. This is an indication that these residues might be flexible when inhibitor or substrate is not present in the active site although they are not in direct contact to inhibitor, NADPH or residues from the flexible lid.

These observations are consistent with the kinetic mechanism of the enzyme (Jordan et al., unpublished results). THNR follows an ordered ternary complex mechanism, with NADPH binding first, followed by the naphtol substrate. After conversion into the products, vermelone is released first and finally $NADP^+$. This mechanism requires that the lid does not close upon binding of NADPH but has to enable access of the second substrate before the active site is made inaccessible for water during hydride transfer.

Acknowledgements: This work was supported by a grant from the Magnus Bergvall foundation to Y.L. G.S. acknowledges receipt of a major equipment grant from the Knut and Alice Wallenberg foundation.

References

[1] Howard, R.J. and Ferrari, M.A. (1989) Exp. Mycol. 13, 403–418.
[2] Vidal-Cros, A., Viviani, F., Labesse, G., Boccara, M. and Gaudry, M. (1994) Eur. J. Biochem. 219, 985–992.
[3] Chumley, F.G. and Valent, B. (1990) Mol. Plant-Microbe Interact. 3, 135–143.
[4] Andersson, A., Jordan, D., Schneider, G. and Lindqvist, Y. (1996) Structure 4, 1161–1170.
[5] Andersson, A., Jordan, D., Schneider, G., Valent, B. and Lindqvist, Y. (1996) PROTEINS: Structure, Function Genetics 24, 525–527.
[6] Otwinowski, Z. (1993) Proceedings of the CCP4 Study Weekend, Daresbury Laboratory, Warrington, UK, pp. 56–62.
[7] Collaborative Computational Project, Number 4 (1994) Acta Cryst. D50, 760–763.
[8] Brünger, A.T., Kuriyan, J. and Karplus, M. (1987) Science 235, 458–460.
[9] Engh, R.A. and Huber, R. (1991) Acta Cryst. A47, 392–400.
[10] Jones, T.A., Zou, J.Y., Cowan, S. and Kjeldgaard, M. (1991) Acta Cryst. A47, 110–119.
[11] Sherrif, S. and Hendrickson, W.A. (1987) Acta Cryst. A43, 118–121.
[12] Navaza, J. (1992) Proceedings of the CCP4 study weekend. (Dodson, E.J., Gower, S., Wolf, W., eds.), SERC, UK 87–91.
[13] Laskowski, R.A., MacArthur, M.W., Moss, D.S. and Thornton, J.M. (1993) J. Appl. Cryst. 26, 946–950.
[14] Bystroff, C., Oatley, S.J. and Kraut, J. (1990) Biochemistry 29, 3263–3277.
[15] Kraulis, P.J. (1991) J. Appl. Cryst. 24, 946–950.